



ORIGINAL ARTICLE

# Electrophysiological features of sleep in children with Kir4.1 channel mutations and Autism–Epilepsy phenotype: a preliminary study

Federico Cucchiara<sup>1,2,\*</sup>, Paolo Frumento<sup>3</sup>, Tommaso Banfi<sup>4</sup>, Gianluca Sesso<sup>5</sup>, Marco Di Galante<sup>6</sup>, Paola d’Ascanio<sup>1</sup>, Giulia Valvo<sup>7</sup>, Federico Sicca<sup>6</sup> and Ugo Faraguna<sup>1,6</sup>

<sup>1</sup>SONNOLab, Department of Translational Research and of New Surgical and Medical Technologies, University of Pisa, Pisa, Italy, <sup>2</sup>Clinical Pharmacology and Pharmacogenetic Unit, Department of Clinical and Experimental Medicine, University of Pisa, Pisa, Italy, <sup>3</sup>Unit of Biostatistics, Institute of Environmental Medicine, Karolinska Institutet, Stockholm, Sweden, <sup>4</sup>The BioRobotics Institute, Scuola Superiore Sant’Anna, Pontedera, Italy, <sup>5</sup>Neuropsychiatry Complex Unit, Department of Clinical and Experimental Medicine, University of Pisa, Pisa, Italy, <sup>6</sup>Department of Developmental Neuroscience, IRCCS Stella Maris Foundation, Pisa, Italy, and <sup>7</sup>Child and Adolescent Neuropsychiatric Unit, Azienda USL Toscana Sudest, Grosseto, Italy

\*Corresponding author. Federico Cucchiara, Via Roma, 55; 56126, Pisa (PI), Italy. Email: [f.cucchiara1@studenti.unipi.it](mailto:f.cucchiara1@studenti.unipi.it); [fed.cuc1@gmail.com](mailto:fed.cuc1@gmail.com)

## Abstract

**Study Objectives:** Recently, a role for gain-of-function (GoF) mutations of the astrocytic potassium channel Kir4.1 (KCNJ10 gene) has been proposed in subjects with Autism–Epilepsy phenotype (AEP). Epilepsy and autism spectrum disorder (ASD) are common and complexly related to sleep disorders. We tested whether well characterized mutations in KCNJ10 could result in specific sleep electrophysiological features, paving the way to the discovery of a potentially relevant biomarker for Kir4.1-related disorders.

**Methods:** For this case–control study, we recruited seven children with ASD either comorbid or not with epilepsy and/or EEG paroxysmal abnormalities (AEP) carrying GoF mutations of KCNJ10 and seven children with similar phenotypes but wild-type for the same gene, comparing period–amplitude features of slow waves detected by fronto–central bipolar EEG derivations (F3–C3, F4–C4, and Fz–Cz) during daytime naps.

**Results:** Children with Kir4.1 mutations displayed longer slow waves periods than controls, in Fz–Cz (mean period = 112,617 ms ± SE = 0.465 in mutated versus mean period = 105,249 ms ± SE = 0.375 in controls,  $p < 0.001$ ). An analog result was found in F3–C3 (mean period = 125,706 ms ± SE = 0.397 in mutated versus mean period = 120,872 ms ± SE = 0.472 in controls,  $p < 0.001$ ) and F4–C4 (mean period = 127,914 ms ± SE = 0.557 in mutated versus mean period = 118,174 ms ± SE = 0.442 in controls,  $p < 0.001$ ).

**Conclusion:** This preliminary finding suggests that period–amplitude slow wave features are modified in subjects carrying Kir4.1 GoF mutations. Potential clinical applications of this finding are discussed.

**Key words:** children; autism; epilepsy; EEG; nap; sleep homeostasis; tripartite synapse; K<sup>+</sup> buffering; Kir4.1; KCNJ10

## Statement of significance

An increasing body of experimental evidence suggests an association between sleep and neurodevelopmental disorders such as autism spectrum disorders (ASDs) and epilepsy/EEG paroxysmal abnormalities. Furthermore, a recent study has highlighted a possible link between the concurrence of these two disorders (AEP, Autism–Epilepsy phenotype) and mutations in the KCNJ10 gene coding for the astrocytic potassium channel Kir4.1. This preliminary study reports on electrophysiological sleep features observed in children with ASD or AEP and gain-of-function mutations of Kir4.1, which can be used as possible biomarkers of Kir4.1 dysfunction in these disorders.

Submitted: 16 March, 2019; Revised: 17 September, 2019

© Sleep Research Society 2019. Published by Oxford University Press [on behalf of the Sleep Research Society].

This is an Open Access article distributed under the terms of the Creative Commons Attribution-NonCommercial-NoDerivs licence (<http://creativecommons.org/licenses/by-nc-nd/4.0/>), which permits non-commercial reproduction and distribution of the work, in any medium, provided the original work is not altered or transformed in any way, and that the work is properly cited. For commercial re-use, please contact [journals.permissions@oup.com](mailto:journals.permissions@oup.com)

## Introduction

### Autism–epilepsy phenotype (AEP)

Autism spectrum disorders (ASDs) are a broad group of neurodevelopmental disorders characterized by impaired communication and social interactions and repetitive and restrictive behaviors [1] that begin in childhood, with a variable degree of severity, and are associated with variable impairments in cognitive functioning [2]. Etiologies and neural alterations underlying ASD are not clear and are still highly debated [3–7].

ASDs are strongly associated with epilepsy and/or paroxysmal EEG abnormalities. Epidemiologically, people with ASD (especially females with lower verbal and nonverbal abilities [8]) have a significantly higher risk of developing epilepsy, with a prevalence ratio of around 30%; conversely ASD features can be found in 5% of patients suffering from epilepsy [8, 9]. Yet, individuals with autism and comorbid epilepsy have lower intellectual, speech, and language abilities as compared to those without epilepsy [8].

The relationship between ASD and epilepsy/paroxysmal EEG abnormalities has long been known, but common pathophysiological aspects have only recently been systematically described [10] in a subgroup of individuals displaying AEP [11, 12].

### Astrocytic Kir4.1 channels gain-of-function defects are related to autism–epilepsy comorbidity

A recent study [11] has revealed that the dysfunction of the astrocytic inwardly-rectifying potassium channels Kir4.1 (encoded by the *KCNJ10* gene) represents a possible pathogenic mechanism contributing to ASD and epilepsy comorbidity. Three *KCNJ10* gain-of-function (GoF) mutations (p.R18Q, p.V84M, and p.R348H) have showed a significant correlation with a relatively benign outcome of seizures, lower frequency of stereotyped behaviors, and greater alteration of sensory perception in AEP children.

In vitro studies [13–17] clarified the effects of Kir4.1 mutations on channel function: p.R18Q mutation (the most frequent variant found in AEP patients) resulted in an increase in channel expression on astrocytic membranes, whereas the rarer p.R348H and p.V84M variants were instead associated with lower sensitivity to intracellular acidification and increased single channel conductance, respectively. The gain of Kir4.1 function ultimately led to an increase in K<sup>+</sup> buffering by astrocytic cells, especially when exposed to high extracellular K<sup>+</sup> concentration.

K<sup>+</sup> buffering in astrocytes is an essential mechanism for the maintenance of optimal extracellular K<sup>+</sup> concentration and consequently represents a crucial process for correct synaptic functioning [18–20] and regulation of neuronal excitability [21]. Kir4.1 activity at the tripartite synapse also plays an important role in synaptic plasticity by mediating neurovascular coupling [22] and promoting synaptic maturation and remodeling [23] that occur during sleep and across neurodevelopment. Altered synaptic homeostasis due to dysfunction of the Kir4.1 channel may therefore contribute to epileptic seizures and to cognitive and behavioral deficits [24, 25].

### Sleep and AEP

A high prevalence of sleep disorders has been found in ASD patients with significant consequences on daytime behavior [26, 27] and overall quality of life and a major impact on externalizing symptoms [10]. Among the most commonly reported sleep

problems, initial, intermediate, and terminal insomnias, and different parasomnias such as sleepwalking, REM sleep disorders, and sleep paralysis are described [25, 26]. Also, epilepsy and sleep have a significant mutual influence, such that sleep states can affect epilepsy, and in turn epilepsy can affect sleep [28, 29]. Indeed changes in membrane potential and in ion channels activity at the cellular level that occur in wakefulness-to-sleep transitions constitute a fertile ground for the expression of epileptic phenomena [29]. Moreover, sleep deprivation has a strong epileptogenic effect especially in association with physical or emotional stress. Finally, seizures and anticonvulsant therapy can alter sleep architecture [28, 30].

Within sleep deepening, while cerebral cortex disconnects from the external environment, the most distinctive electrophysiological feature is the occurrence of slow waves (0.5–4 Hz) in all or most cortical areas [31]: they are negative deflections followed by positive peaks, which cross the x-axis with a certain inclination [32–34].

Every wave originates in small different regions of the cortex and travels uniquely to other cortical areas with its own speed and pattern of propagation, often originating in anterior cortical regions and propagating throughout the mesial highway to posterior regions [32, 33, 35].

Slow waves are the consequence of the activity of million bistable neurons around cortical layer 5 [36, 37] that nearly every second (<1 Hz) [35] generate synchronized membrane potentials slow oscillations, from hyperpolarized “down-states” during which neurons remain silent for a few hundred milliseconds, to “up-states” characterized by prolonged depolarization and irregular firing [38–41]. Mechanisms that trigger and terminate up- and down-states remain unclear, but the importance of depolarization-dependent K<sup>+</sup> currents [42, 43] is wellknown: since K<sup>+</sup> is necessary to modulate neuronal excitability both at the presynaptic and postsynaptic levels, the ability of neuroglia to buffer local increases of extracellular K<sup>+</sup> confer to these cells an active role in the modulation and spreading of cortical oscillatory activities [44].

Changes in slow wave parameters point out changes in synchrony of neuronal firing which in turn reflect changes in synaptic strength and efficiency of cortico-cortical connections [33, 45, 46]. While slow wave amplitude correlates to the number of neurons entering synchronously in the up- or down-state, slow wave slope reflects the speed of neuronal recruitment [41, 43]. Thus, slow waves amplitude and slope act as indirect but reliable EEG markers of circuit dynamics, which in turn may be expression of synaptic plasticity [33, 42, 47, 48].

During neuronal development, changes in slow wave parameters reflect unique aspects of brain connectivity and adaptation during synaptic maturation [46, 49, 50]. Throughout adolescence, a progressive weakening of short-range connections occurs in association with a strengthening of long-range ones [51], resulting in a significant decline of the slow wave activity (SWA) [52–54].

Instead, in individuals with autism, circuits involving nearby neurons are more frequently activated than those involving neurons among distant cortical areas [55], so that the former would be consolidated while the latter would have been lost permanently [56]. This impairment of down-selection during critical developmental periods could have irreversible consequences on wiring and function of neural circuits [57–60] and could reflect in major sleep abnormalities [27, 46].

Altered sleep-wake cycles have implications on astrocytic plasticity, too [23, 61, 62]. Astrocytes are responsive to changes in

wake-promoting neuromodulators, not only by regulating extracellular volume but also by influencing composition and glymphatic drainage of interstitial fluid. These events are accompanied by changes in astrocyte–neuron interactions and neurovascular coupling, synaptic maturation and remodeling, and especially neuronal discharge patterns [63]. Reduced astrocytic coverage during sleep may favor glutamate spill-over and increase K<sup>+</sup> buffering, which promote neuronal synchronization during NREM sleep [61, 63, 64] and characterize EEG slow wave sleep pattern [21, 44, 65].

In this study, we compared several parameters of slow waves in a group of seven mutated children and in seven sex- and age-matched control subjects, to test our hypothesis that a well characterized mutation in Kir4.1 channels and consequent and persistent K<sup>+</sup> buffering could result in specific electrophysiological features of sleep (amplitude, period, and down and up slope), paving the way to the discovery of potentially clinically relevant biomarkers that may help in distinguishing children with ASD/AEP and GoF mutations of astrocytic Kir4.1 channel from those with similar phenotypes but no Kir4.1 dysfunction.

## Methods

### Subjects

Fourteen subjects with ASD were included in the present study, 12 males and 2 females ranging from 3 to 13 years of age (8.25 mean ± 3.54 SD). Twelve of them (10 males and 2 females) had

a history of epileptic seizures and/or EEG abnormalities, and among them, 5 (4 males) were taking sodium valproate (VPA) during EEG recording. Seven subjects of our cohort (6 males), carried a GoF mutation of the Kir4.1 channel gene. Among them, the R18Q variant was found in 6 males, while the R348H variant was found only in one female. Mutated and control subjects were matched for phenotype, age, and gender (Table 1).

### Recruitment criteria

A cohort of children with ASD/AEP was recruited at the Stella Maris Foundation Hospital from 2009 to 2017. Among them, subjects with a history of seizures and/or EEG abnormalities were included in the autism–epilepsy phenotype subgroup.

Phenotype characterization was carried out through clinical and laboratory assessments, EEG study, and brain magnetic resonance imaging. A family history for epilepsy or ASD was investigated up to the 4th degree of kinship. Clinical and EEG assessments, and *KCNJ10* sequencing, were performed after having obtained an informed consent from parents or caregivers, and complying with the ethical principles outlined by the Declaration of Helsinki.

### EEG recording and sleep scoring

Digital video-EEG-polysomnographic (PSG) systems (Grass Technologies, Rhode Island, United States; Micromed, Mogliano

Table 1. Sample characteristics

ID	Gender: 1=Fml, 2=Ml		Age	Treatment at the time of the EEG under investigation	KCNJ10 mutation	History of seizures 0=No, 1=Yes	Type of seizures	Seizure outcome	Eeg abnormalities 0=No, 1=Yes
1	2		12 years 8 months	VPA	R18Q	1	absences	Remission under VPA	1
2	2		13 years 5 months	-	R18Q	0			1
3	1		9 years 7 months	-	R348H	1	spasms	Spontaneous remission after a febrile illness	1
4	1		8 years 7 months	VPA	WT	1	absences	Remission under VPA	1
5	2		12 years 8 months	VPA	WT	1	focal	Remission under VPA	1
6	2		3 years 8 months	-	R18Q	0			0
7	2		3 years 9 months	-	WT	0			0
8	2		6 years 3 months	-	R18Q	1	Spasms + focal	Remission under ACTH, VPA, TPM	1
9	2		6 years 0 months	-	R18Q	1	spasms	Remission under ACTH and VPA	1
10	2		5 years 6 months	-	R18Q	0			1
11	2		6 years 4 months	VPA	WT	1	focal	Still active epilepsy	1
12	2		6 years 9 months	VPA	WT	1	tonic-clonic	Remission under VPA	1
13	2		13 years 3 months	-	WT	0			1
14	2		5 years 8 months	-	WT	0			1

ID= identification number; Fml= female; Ml= male; VPA= sodium valproate; WT= Wild Type.

Veneto, Italy) were used to obtain sleep recordings in children during 1-h-long daytime naps on average (Table 2). PSG measurements included 19 electrodes EEG in a standard 10–20 location, deltoid muscle electromyogram (EMGs), and electrocardiogram (ECG).

Sleep recordings were scored by a trained scorer according to *American Academy of Sleep Medicine* (AASM) standardized criteria [28]: Alice Sleepwear software was used for manual visual epoch-by-epoch scoring on 30-s-long segments of neurologic layout of PSG channels.

### Slow wave detection and analysis of wave parameters

For slow wave sleep detection a single EEG signal channel was used, as performed in a recent study [66]. The choice was based both on methodological and electrophysiological rationales. Each derivation was preliminarily assessed for every subject. For each derived signal we performed temporal and spectral analyses and a score, from 0 to 10, was then assigned to judge the quality and cleanliness of each subject's signal. Thus, for each signal, the scores ranged from 0 to 140 given that there were 14 subjects in total. F3-C3 (107 points), F4-C4 (103 points) and Fz-Cz (108 points) were the most eligible channels for evaluation. First, the Fz-Cz channel was selected since it was the one with few artifacts and the most evident waves and it is considered the most suitable for evaluating slow waves [67, 68]; then, to enrich the dataset and support the results, the same analyses were also re-run separately for F3-C3 and F4-C4 since they were of almost equivalent quality and equivalent artifacts-free.

Sleep slow waves were automatically detected using a re-edited EEGLAB toolbox (MatLab, The Math Works Inc., Natick, MA). First, 200 Hz sampled signal was high-pass filtered (0.1 Hz) and band-pass filtered (0.3–30 Hz) to remove artifacts and background noise. Second, using a Chebyshev Type II filter (band-pass 0.5–4.0 Hz, stopband 0.1 and 10 Hz) signal was re-filtered for slow wave best detection. The filter parameters were visually optimized on the EEG signal to achieve minimal wave shape and amplitude distortion while allowing the least high-frequency contamination.

Finally, individual half-waves were detected by defining a half-wave as negative deflections between 2 zero-crossings [69]. The zero-crossing detection was chosen for the analysis due to the high degree of variability in the positive signal deflections compared to the stability of the negative deflections.

Within an artifact- and epileptic abnormalities-free NREM epoch, only half-waves whose period and maximal negative amplitude were bigger than the mode of all half-waves detected were considered as slow waves.

The use of the mode as a threshold was empiric, carefully assessed by analyzing each subject after applying the same

criteria. The mode was assessed for period and amplitude as the highest peak of a histogram, which in turn is the frequency distribution in classes of a parameter.

Moreover, to assess whether differences in slow wave amplitude are related to difference in slow wave period, we detected sleep slow waves based only on a duration criterion, for instance, 0.25–1 s negative-to-positive zero crossing.

This detection procedure described above has been found to be similar to that employed in a previous work on period-amplitude analysis [33, 70] and allowed a specific detection of slow waves during NREM2 and NREM3 stages sleep. Identified slow waves were then plotted to visually assess the reliability of the automatic detection for each subject.

For every detected slow oscillation, we collected several single-wave parameters that could be used to compare the two groups: (1) half-waves number, (2) half-waves period, (3) amplitudes of the maximal negative peaks, and (4) maximal half-wave down and up slope. Maximal slopes were defined as the maximum of the signal derivative following the negative zero crossing but before the most negative peak (down slope), or after the most negative peak but prior to the positive-going zero crossing (up slope).

To improve slow waves detection and to avoid detection of large epileptic waves like slow waves (EEG abnormalities highlighted in 12/14 subject, 64.29%), MatLab scripts have been implemented based on a previous work by Dr. Brady Riedner of University of Wisconsin (Madison, WI) [33] (Figure 1).

Finally, since the vast majority of the recorded waves had an amplitude <100  $\mu$ V (95.76% of wild-type subjects' waves, 98.32% of mutated subjects' ones), we focused on slow wave parameters within this amplitude range and subdivided detected waves showing an amplitude <100  $\mu$ V into 10 groups of 10  $\mu$ V of width.

However, since subject 13's data showed multiple artifactual epileptic graphoelements that affected the majority of the EEG tracing, we excluded subject 13 and the paired control subject 2 from the analysis of slow waves.

### Statistical analysis

Statistical analyses were performed using Sigma Plot software to compare ASD/AEP children with astrocytic Kir4.1 mutated channels to a control group of ASD/AEP wild-type (WT) children.

Each comparison was performed between all mutations and all WT, then between mutated and WT subgroups matched by age, to evaluate the specific effect of this variable on sleep.

For each parameter, comparisons were first performed between the two groups of mutated and WT children; then, age- and sex-matched pairs of mutated and WT children were individually compared to estimate the effect size of related clinical variables.

Table 2. Sleep measures for entire nap

	Wild-Type	Mutated	P-value
Total time in bed, min	54.14 $\pm$ 3.776	60.57 $\pm$ 3.884	0.258
Total sleep time (TST), min	24.71 $\pm$ 2.286	22.00 $\pm$ 2.177	0.407
NREM1, min	1.64 $\pm$ 0.497	1.86 $\pm$ 0.652	0.798
NREM2, min	8.57 $\pm$ 1.706	8.86 $\pm$ 2.593	0.928
NREM3, min	13.50 $\pm$ 3.677	10.43 $\pm$ 2.494	0.503
Waking period	1.36 $\pm$ 0.322	0.86 $\pm$ 0.210	0.218

Data are expressed as mean  $\pm$  SEM ( $n = 7$ ). Two subjects do not have NREM 3 sleep stage. None of all presents REM sleep stage. min, minutes; NREM, nonrapid eye movement; SEM, standard error of the mean;  $n$ , number of subjects per group.

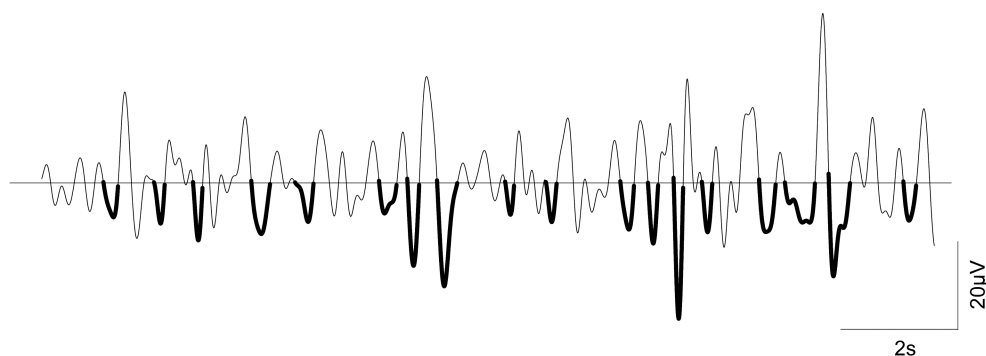


**Figure 1.** Slow waves detection. A MatLab® EEG plot of a NREM3 sleep epoch is here reported. Amplitude detected half-slow waves are highlighted with a thick black line, whereas the background rhythm is marked with a fine one. Half-waves were defined as negative deflections between 2 zero-crossings. Slow waves were automatically detected using MatLab EEGLAB toolbox, editing a previous detection algorithm described by Riedner et al. [33].

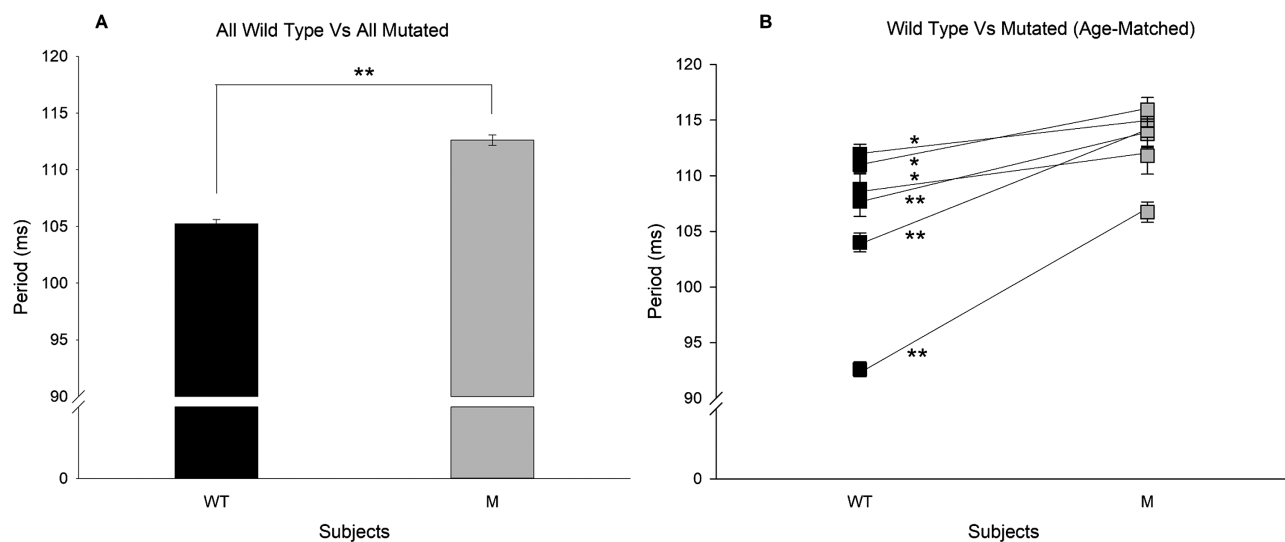


**Figure 2.** Slow wave period in a case-control analysis. (A) Period (ms) is shown on y-axis. WT ( $n = 10,390$  waves) bar is reported in anthracite/black while M ( $n = 7,696$  waves) one is in gray. Error bars are also represented. (B) Period (ms) is shown on y-axis. WT box-plots are reported in anthracite/black while M ones are in gray. Mutated subjects have slow waves with longer periods than WT and also in all age-matched comparisons differences are greater than would be expected by chance. \* $p < 0.05$ ; \*\* $p < 0.001$ ; WT, wild type; M, mutated; ms, milliseconds;  $n$ , number of waves.

A nonparametric Mann–Whitney U-test was performed to assess differences in slow wave parameters. Finally, to take into account the effect of potential confounders, we estimated longitudinal linear regression using two different methods: random-effects (RE) and generalized estimating equations (GEE) models.

## Results

First, we compared total sleep and sleep stage durations between mutated children group and controls (Table 2).

There were no significant differences in total time in bed, total sleep time (TST), NREM1, NREM2, NREM3 and in waking epochs occurring during nap, between WT and mutated subjects.

### Astrocyte Kir4.1 channel mutation is associated with longer slow waves period

In order to examine changes in individual slow wave parameters between WT and mutated subjects, we analyzed a statistically comparable number of automatically detected slow waves in the Fz-Cz derivation (median number of detected slow waves in

mutated subjects = 1724 versus median number of detected slow waves in control subjects = 1309.5, Wilcoxon Test  $p$ -value = 0.313). A significant difference was observed in the period of the half-negative waves between cases and controls. First, we found that the slow waves period in mutated subjects was longer than the wild types' one (mean period =  $112,617 \text{ ms} \pm \text{SE} = 0.465$  in mutated versus mean period =  $105,249 \text{ ms} \pm \text{SE} = 0.375$  in controls,  $p < 0.001$ ). Then, age- and sex-matched pairs of mutated and WT children, ranging from 3 to 13 years, were created to compare sleep slow waves parameters and avoid confounding factors due to changes across neurodevelopment (Figure 2).

For each couple we normalized the interval duration of detection window of slow waves on the shortest one between the two subjects within the couple. So, a difference in slow wave form is shown between cases and controls (Figure 3).

Also, we found that the difference between mutated and WT subjects is further enhanced in the range from  $-10 \mu\text{V}$  to  $-40 \mu\text{V}$ . Within this range, the period was significantly longer in subjects with astrocyte Kir4.1 mutated channels compared to controls. Conversely, higher amplitude slow waves have shown no statistically significant difference between cases and controls (Figure 4).

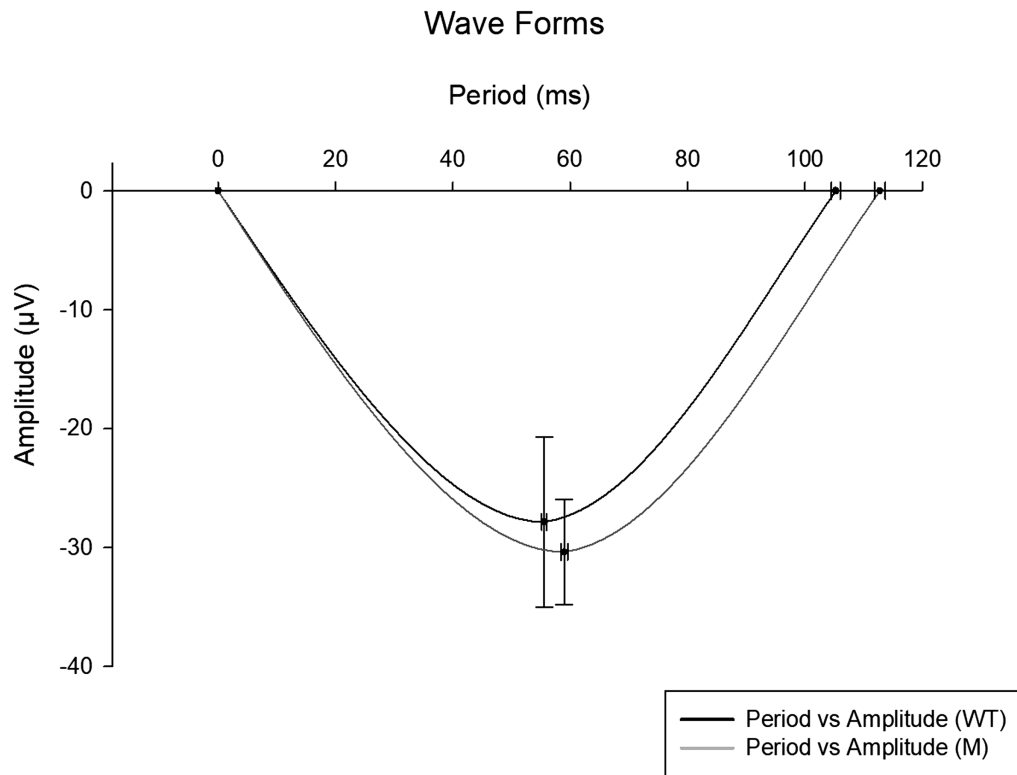


**Figure 3.** Wave forms. Here is a graphical representation of the comparison between the average waveform in WT children (anthracite/black) and the average waveform in Kir4.1-mutated children (gray). Period (ms) and amplitude ( $\mu\text{V}$ ) are, respectively, shown on the x-axis and on the y-axis. The standard errors are also shown for mean amplitude of the negative peaks, mean time of the negative peaks and mean period.

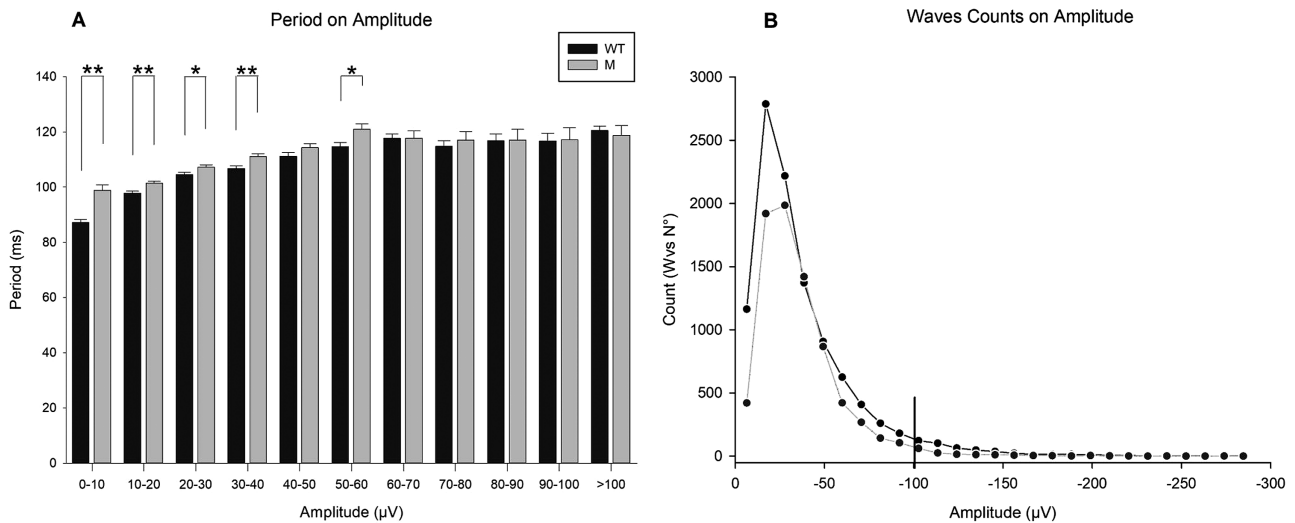


**Figure 4.** Slow wave period in an amplitude-dependent case-control analysis. (A) Amplitude ( $\mu\text{V}$ ) and period (ms) are, respectively, shown on x-axis and y-axis. WT bars are reported in anthracite/black while M bars are in gray. Error bars are represented, too. We analyzed the trend of the period according to amplitude of the maximal negative peaks of the detected half-slow waves. We analyzed the data by evaluating an amplitude range between 0 and 100  $\mu\text{V}$  in which the greatest number of waves is recorded (as shown in B). This range has been further subdivided into subranges of 10  $\mu\text{V}$ . We found statistically significant differences between the two groups in the ranges between 0 and 40  $\mu\text{V}$  and from 50  $\mu\text{V}$  to 60  $\mu\text{V}$ . \*  $p < 0.05$ ; \*\*  $p < 0.001$ ; WT, Wild Type; M, mutated; ms, milliseconds;  $\mu\text{V}$ , microvolts; Wvs N, waves number.

An analogue result was obtained for F3-C3 (mean period = 125,706 ms  $\pm$  SE = 0.397 in mutated versus mean period = 120,872 ms  $\pm$  SE = 0.472 in controls,  $p < 0.001$ ) and F4-C4 (mean period = 127,914 ms  $\pm$  SE = 0.557 in mutated versus mean period = 118,174 ms  $\pm$  SE = 0.442 in controls,  $p < 0.001$ ) (Figures 5 and 6).

#### Astrocyte Kir4.1 channel mutation is not associated with other changes in slow waves parameters

Similarly, we analyzed down and up slope of slow waves detected in Fz-Cz signals, both between groups and among age-matched couples. Significant differences emerged in slow wave slopes between age-matched couples of mutated and WT subjects (mean

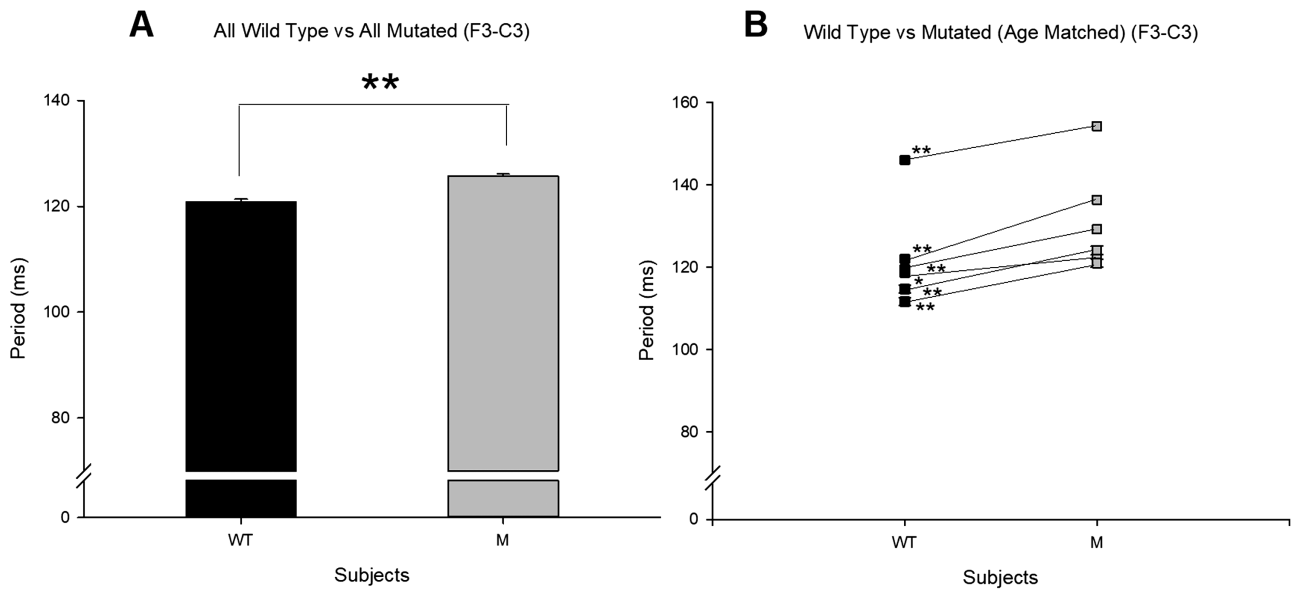


**Figure 5.** Slow wave period in a case-control analysis; F3-C3 derivation. (A) Period (ms) is shown on y-axis. WT ( $n = 7,740$  waves) bar is reported in anthracite/black while M ( $n = 13,346$  waves) one is in gray. Error bars are also represented. (B) Period (ms) is shown on y-axis. WT box-plots are reported in anthracite/black while M ones are in gray. Mutated subjects have slow waves with longer periods than WT and also in all age-matched comparisons differences are greater than would be expected by chance. \*  $p < 0.05$ ; \*\*  $p < 0.001$ ; WT, wild type; M, mutated; ms, milliseconds; n, number of waves.

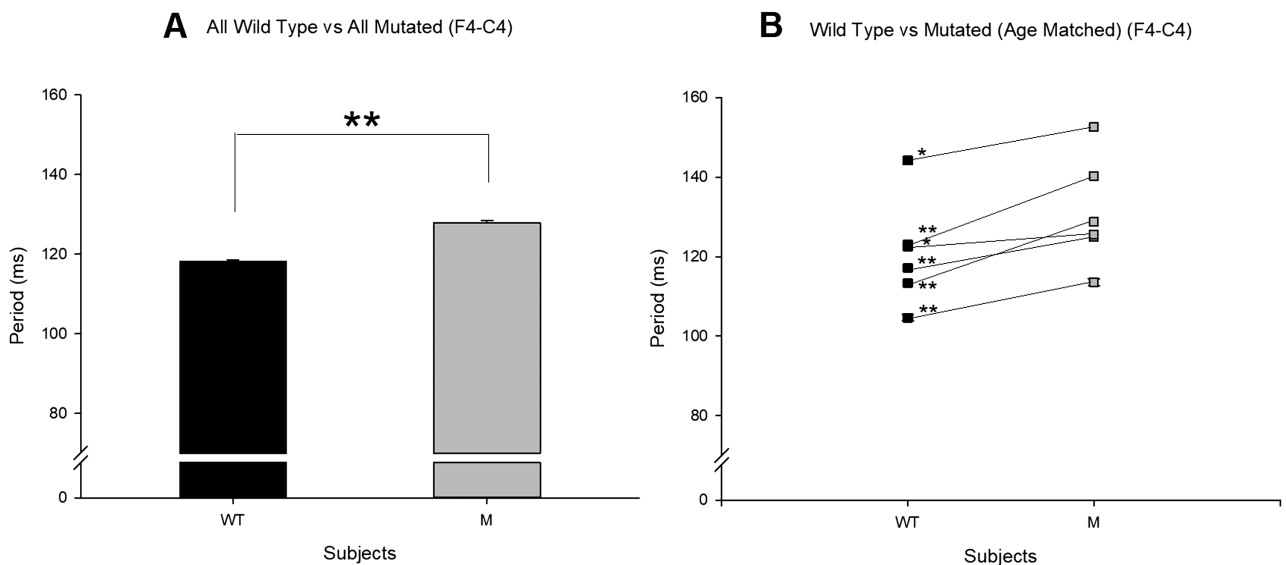


**Figure 6.** Slow wave period in a case-control analysis; F4-C4 derivation. (A) Period (ms) is shown on y-axis. WT ( $n = 9,217$  waves) bar is reported in anthracite/black while M ( $n = 7,028$  waves) one is in gray. Error bars are also represented. (B) Period (ms) is shown on y-axis. WT box-plots are reported in anthracite/black while M ones are in gray. Mutated subjects have slow waves with longer periods than WT and also in all age-matched comparisons differences are greater than would be expected by chance. \*  $p < 0.05$ ; \*\*  $p < 0.001$ ; WT, wild type; M, mutated; ms, milliseconds; n, number of waves.

down-slope =  $500,669 \mu\text{V}/\text{ms} \pm \text{SE} = 3.643$  in mutated versus mean down-slope =  $519,857 \mu\text{V}/\text{ms} \pm \text{SE} = 4.306$  in controls,  $p \leq 0.001$ ; mean up-slope =  $493,835 \mu\text{V}/\text{ms} \pm \text{SE} = 3.591$  in mutated versus mean up-slope =  $491,824 \mu\text{V}/\text{ms} \pm \text{SE} = 3.644$  in controls,  $p \leq 0.001$ ; however, the distribution of slow waves slopes mean values is highly variable depending on the age and no meaningful trend is observed between cases and controls (Figures 7 and 8).

In the end, although we found that in the fronto-central medial bipolar derivation (Fz-Cz) the overall mean of slow waves amplitude was significantly higher in mutated subjects than controls, the result does not reflect a marked difference between the slow waves amplitudes detected in KCNJ10 mutated and WT

subjects (mean amplitude =  $-30,371 \mu\text{V} \pm \text{SE} = 4.4282$  in mutated versus mean amplitude =  $-27,854 \mu\text{V} \pm \text{SE} = 7.167$  in controls,  $p \leq 0.001$ ) and no meaningful trend is observed between cases and controls across ages (Figure 9).

The results seem to be confirmed also estimating longitudinal linear regression using both the RE and GEE methods (Table 3).

## Discussion

Our study aimed at evaluating electrophysiological features of sleep in a cohort of ASD/AEP children with GoF mutation of the astrocytic Kir4.1 channel, compared to age- and sex-matched

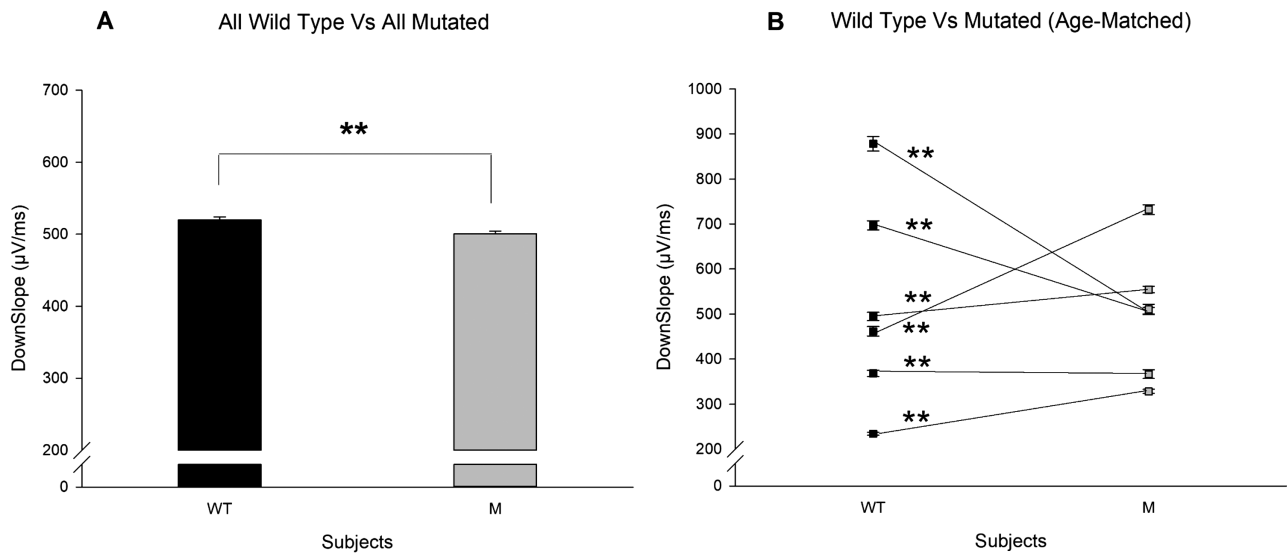


**Figure 7.** Down-slope in a case-control analysis. (A) Down-slope ( $\mu\text{V}/\text{ms}$ ) is shown on y-axis. WT ( $n = 10,390$  waves) bar is reported in anthracite/black while M ( $n = 7,696$  waves) one is in gray. Error bars are also represented. (B) Down-slope ( $\mu\text{V}/\text{ms}$ ) is shown on y-axis. WT box-plots are reported in anthracite/black while M ones are in gray. Using Mann-Whitney rank-sum test we found statistically significant differences between slow waves. Down-slopes of every subject with mutated Kir4.1 channels compared with its own WT control matched by age.  $**p < 0.001$ ; WT, wild type; M, mutated; ms, milliseconds;  $\mu\text{V}$ , microvolts; n, number of waves.

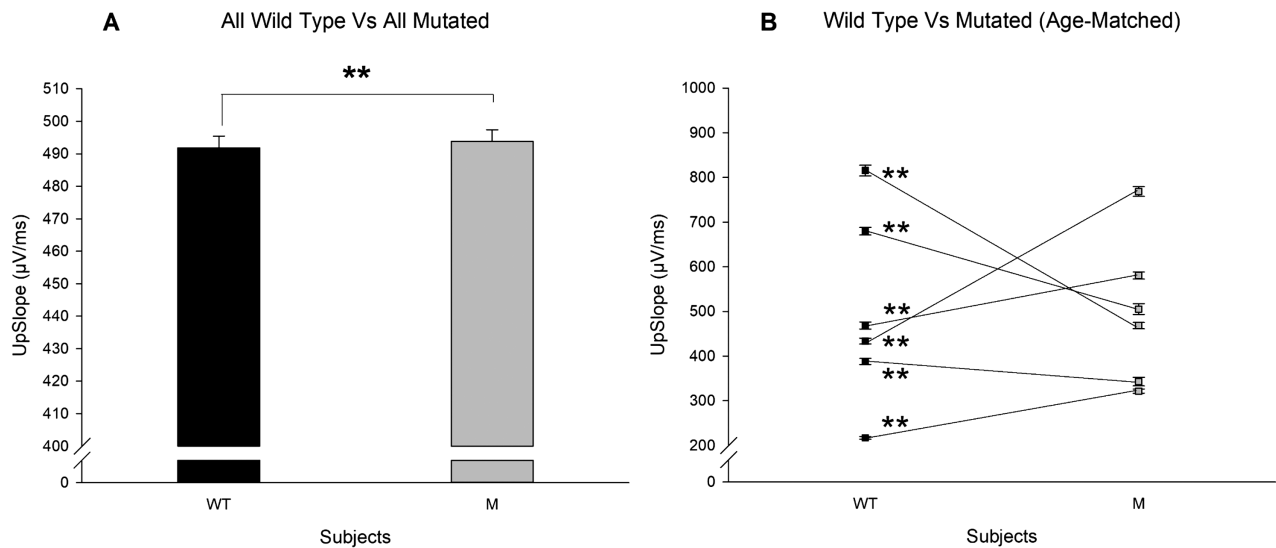


**Figure 8.** Up-slope in a case-control analysis. (A) Up-slope ( $\mu\text{V}/\text{ms}$ ) is shown on y-axis. WT ( $n = 10,390$  waves) bar is reported in anthracite/black while M ( $n = 7,696$  waves) one is in gray. Error bars are also represented. (B) Up-slope ( $\mu\text{V}/\text{ms}$ ) is shown on y-axis. WT box-plots are reported in anthracite/black while M ones are in gray. Using Mann-Whitney Rank Sum Test we found statistically significant differences between slow waves Down-slopes of every subject with mutated Kir4.1 channels compared with its own WT control matched by age.  $**p < 0.001$ ; WT, wild type; M, mutated; ms, milliseconds;  $\mu\text{V}$ , microvolts; n, number of waves.

children with similar phenotypes, but not carrying Kir4.1 mutations. Although the ASD/AEP children cohort was small, subjects were recruited over a long period of time (from 2009 to 2017) and are the only ones who are recognized—at least to date—to have an association between ASD/AEP and GoF mutation of the astrocytic Kir4.1 channels. This study, to the best of our knowledge the first investigating sleep EEG features in this cohort, reveals that the slow waves detected in sleep EEG recordings during daytime naps behave differently when associated with mutations in Kir4.1 channels and consequent dysfunction of astrocytic  $\text{K}^+$  buffering [11]. Subjects with Kir4.1 mutations have indeed a significantly longer slow waves period than controls. This difference, which is particularly relevant for slow waves in the low-amplitude range, appears to be independent from the

developmental stage since it remains stable from childhood to adolescence, thus providing a potential electrophysiologically grounded noninvasive biomarker for these mutations.

One might further speculate on the pathogenic mechanism underlying these alterations. Indeed, the local increase in extracellular  $\text{K}^+$  has an active role in the homeostasis of neuronal excitability [21, 44] but the mutations of *KCNJ10* might prevent this increase by favoring a strongest or more continuous  $\text{K}^+$  buffering that is collected from astrocytes and carried to other distant brain areas [20].

Therefore, in subjects with mutated Kir4.1 channels the increase in period duration might reflect a longer time during slow wave sleep in a state of hyperpolarization (down-state) which is in turn reflected by a longer negative half-wave period [71].

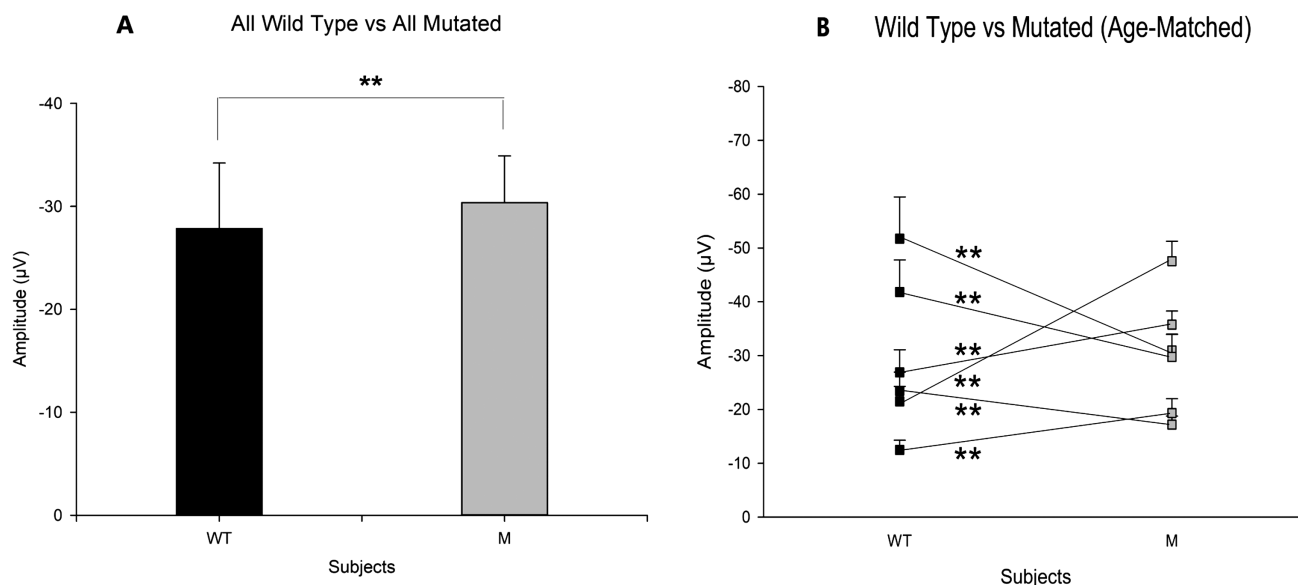


**Figure 9.** Amplitude case-control analysis. (A) Amplitude ( $\mu\text{V}$ ) is shown on y-axis. Wild Type (WT,  $n = 10,390$  peaks) bar is reported in anthracite/black while mutated (M,  $n = 7,696$  peaks) is in gray. Error bars are also represented. Amplitude evaluation in a stand-alone manner shows a statistically significant difference between the 2 groups. (B) Amplitude ( $\mu\text{V}$ ) is shown on y-axis. WT box-plots are reported in anthracite/black while M ones are in gray. Using Mann-Whitney rank-sum test we found statistically significant differences between slow waves Amplitudes of every subject with mutated Kir4.1 channels compared with its own WT control matched by age.  $**p < 0.001$ ; WT, wild type; M, mutated;  $\mu\text{V}$ , microvolts;  $n$ , number of waves.

**Table 3.** Longitudinal linear regression estimation using both the RE and GEE methods

	Crude (RE)	Adjusted (RE)	Crude (GEE)	Adjusted (GEE)
Amplitude	0.834	0.827	0.819	0.773
Down-slope	0.816	0.753	0.799	0.690
Up-slope	0.814	0.810	0.796	0.756
Period	0.037	0.025	0.022	0.015

In this table, the  $p$ -values associated to subjects with mutated KCNJ10 are shown. Two models have been made: one “Crude” including only KCNJ10, and one “Adjusted” in which gender, age and VPA were also included.

RE, random effects model; GEE, generalized estimating equations model; VPA, sodium valproate.

This difference becomes more evident when a small number of neurons is recruited in the oscillatory activities resulting in small amplitude slow waves [45, 46], which are proportionally more sensitive to changes in the extracellular ions concentration.

Thus, the period of slow waves, which is generally modulated by extracellular factors such as the persistent  $\text{Na}^+$  current and the depolarization-activated  $\text{K}^+$  current [33], could be reliably detected in ASD/AEP children carrying GoF Kir4.1 mutations.

Moreover, we could not find any difference between mutated and WT subjects in the slow wave down and up slopes. This is likely due to the evidence that slow wave slope is deeply influenced by the synaptic strength while being less affected by the surrounding extracellular environment [33, 47], notably the extracellular  $\text{K}^+$  concentration, mostly in the high-amplitude range of slow waves [33, 41, 43]: in fact, slow waves amplitude is supposed to be closely linked to the number of neurons recruited in slow oscillations between up and down states [41, 43]. In other words, the greater the number of neurons recruited in the oscillation, the lower the influence of extracellular ion concentration changes on slow wave amplitude; on the other hand, with fewer recruited neurons, changes in astrocyte  $\text{K}^+$  buffering activity is proportionally more influential.

Finally, high variability was found also in the average of slow waves amplitude, and no meaningful trend was observed

between mutated and WT subjects. The lack of any statistical difference between cases and controls in terms of slow wave parameters other than the period supports the specificity and distinctive role of this electrophysiological feature in the discrimination between mutated and WT subjects.

Furthermore, we could not detect any significant difference between groups in TST, sleep stage duration, and other macrostructural sleep parameters. This further supports the hypothesis that period-amplitude differences in slow wave sleep parameters between cases and controls are likely due to the specific genetic pattern, and consequent  $\text{K}^+$  buffering efficiency, but not to differences in sleep time measures.

Our preliminary results have promising clinical implications since they provide a useful biomarker of Kir4.1 dysfunction in ASD/AEP children harboring KCNJ10 mutations in brief EEG recordings of daytime naps, without needing therefore prolonged EEG monitoring of the sleep. This would avoid the commitment of both medical equipment and technical and health personnel for the entire duration of night EEG recording to highlight sleep disturbance and confirm the phenotype.

The main limit of our study remains the small size of our sample. However, an appropriate statistical approach was used to avoid type 1 errors. We also remark that our sample was heterogeneous with respect to current symptoms and medications

which could create a bias effect in data analysis. As an example, improved Kir4.1 function may decrease seizure propensity [11, 12, 72] and the precise history of seizures could also lead to major changes in synaptic plasticity that may possibly explain the differences observed. We were aware that there were some differences in the two groups analyzed, for instance one patient in the control group (ID 11) still had active epilepsy at the time of the EEG, while all those with Kir4.1 mutations were under remission. Nevertheless, we did our best to match the samples with regard to gender, age, and clinical histories in order to minimize possible biases due to nongenetic features.

Furthermore, the results obtained after evaluating the longitudinal linear regression using both the RE and GEE methods are also quite similar and suggest no significant differences for down slope, up slope and amplitude: intuitively, for these parameters, the differences shown in Figures 7, 8 and 9 could be explained by systematic differences between individuals, whereas a KCNJ10 mutation would not be an important predictor. On the contrary, this is not true for the period, which is confirmed to be significantly influenced by the presence of this mutation (Table 3).

We also tested the strength of the result in the face of a different filter setting (1–3 Hz): re-performing the analyses with these subtle alterations in the choice of filters, we confirmed differences between cases and controls for period (mean period = 130,720 ms  $\pm$  SE = 0.418 in mutated versus mean period = 124,515 ms  $\pm$  SE = 0.412 in controls,  $p$ -value = <0.001), down-slope (mean down-slope = 293,699  $\mu$ V/ms  $\pm$  SE = 2.354 in mutated versus mean down-slope = 304,718  $\mu$ V/ms  $\pm$  SE = 2.762 in controls,  $p$  = 0.003), Up-slope (mean up-slope = 302,264  $\mu$ V/ms  $\pm$  SE = 2.326 in mutated versus mean up-slope = 288,422  $\mu$ V/ms  $\pm$  SE = 2.731 in controls,  $p$   $\leq$  0.001) and amplitude (mean amplitude = -23,707  $\mu$ V  $\pm$  SE = 4.552 in mutated versus mean amplitude = -22,851  $\mu$ V  $\pm$  SE = 6.108 in controls,  $p$  = 0.001).

Given the subtle nature of the results and the low number of subjects, we were careful to repeat the analyses, testing altered half-wave detection criteria too. In estimating longitudinal linear regression using the RE models for slow waves detected with three different setting thresholds, from the least inclusive to the most—mean, median and 95th percentile—we found that while amplitude, down-slope and up-slope are not influenced by the presence of the mutation, differences in the period between cases and controls seem to have a progressive tendency to significance from the mean (“Crude” model  $p$ -value = 0.824; “Adjusted” model  $p$ -value = 0.238) to the 95th percentile (“Crude” model  $p$ -value = 0.032; “Adjusted” model  $p$ -value = 0.039), and through the median (“Crude” model  $p$ -value = 0.191; “Adjusted” model  $p$ -value = 0.077). This is probably due to two reasons: mean and median are most affected by the distribution of values and above all, aberrant or extreme values of the distribution, with respect to the mode; in addition they are less inclusive criteria and many of the waves on which the difference between mutated and wild type is played, are excluded. Similar results were obtained across all fronto-central derivations (Fz-Cz and also F3-C3, F4-C4, data not shown).

The differences in slow wave features should be confirmed by further studies on larger samples of affected subjects in order to verify the reproducibility, specificity, sensitivity and robustness of the present results. ASD and epilepsy are very common worldwide and are clinically important and relevant for public health and socioeconomic burden.

Moreover, sleep has recently emerged as a potential marker of autism and other neurodevelopmental disorders and a close association between epilepsy and sleep has been repeatedly confirmed;

sleep disorders could be so relevant that they might play a causal role in the development of some neuropsychiatric disorders.

Specific sleep abnormalities, repeatedly reported in ASD patients with an epileptic phenotype both clinically and polysomnographically, may play a role for diagnostic purposes.

In our case-control study between ASD/AEP children with mutations of KCNJ10 gene (coding for potassium channels Kir4.1 abundantly expressed in astrocytes) and a control group consisting of children WT for the same gene and similar clinical phenotypes, we compared characteristic parameters of slow waves detected during daytime sleep EEG recordings.

Our hypothesis was that astrocytic Kir4.1 channels GoF mutations and consequent dysfunctional and persistent K<sup>+</sup> buffering could influence neurons activity, slowing down the achievement of their action potential.

This abnormality underlies changes in slow waves features and particularly in period, which is longer in subjects with KCNJ10 mutations compared to WT. This difference in slow wave features could have interesting clinical implications. Evaluation of a short period of a daytime nap is sufficient and more compatible with clinic practice than an entire night sleep recording, providing an instrumental and therefore objective diagnostic support.

The peculiar electrophysiological features of sleep slow waves identified in Kir4.1 mutated children could represent a clinically relevant readout of astrocytic dysfunctions and provide a noninvasive biomarker suitable for monitoring targeted drug therapies in these ASD/AEP patients [11].

## Acknowledgments

We thank Chiara Cirelli, Giulio Tononi and Brady Riedner for helpful advice and discussion.

## Funding

This study was partially supported by Ministero della Salute (Ricerca Corrente to FS and Ricerca Corrente to UF) and the ARPA Foundation (SONNOLab Grant to UF). This was not an industry supported study.

*Conflict of interest statement.* There are no financial conflicts of interest.

## References

- Biondi M, et al. [The Italian edition of DSM-5]. *Riv Psichiatr.* 2014;49(2):57–60. doi:10.1708/1461.16137
- Matson JL, et al. Comorbid psychopathology with autism spectrum disorder in children: an overview. *Res Dev Disabil.* 2007;28(4):341–352.
- Billeci L, et al. On the application of quantitative EEG for characterizing autistic brain: a systematic review. *Front Hum Neurosci.* 2013;7:442.
- Maximo JO, et al. The implications of brain connectivity in the neuropsychology of autism. *Neuropsychol Rev.* 2014;24(1):16–31.
- Conti E, et al. The first 1000 days of the autistic brain: a systematic review of diffusion imaging studies. *Front Hum Neurosci.* 2015;9:159. doi:10.3389/fnhum.2015.00159
- Rizzolatti G, et al. The mirror-neuron system. *Annu Rev Neurosci.* 2004;27:169–192.

7. Thoma P, et al. Empathy and social problem solving in alcohol dependence, mood disorders and selected personality disorders. *Neurosci Biobehav Rev.* 2013;**37**(3):448–470.
8. Bolton PF, et al. Epilepsy in autism: features and correlates. *Br J Psychiatry.* 2011;**198**(4):289–294.
9. Spence SJ, et al. NIH Public Access the role of epilepsy and epileptiform EEGs in autism spectrum disorder. *Dev Neurosci.* 2010;**65**(6):599–606.
10. Hasson CJ, et al. Common neurological co-morbidities in autism spectrum disorders. *Motor Control.* 2009;**27**(4):590–609.
11. Sicca F, et al. Gain-of-function defects of astrocytic Kir4.1 channels in children with autism spectrum disorders and epilepsy. *Sci Rep.* 2016;**6**:34325.
12. Sicca F, et al. Autism with seizures and intellectual disability: possible causative role of gain-of-function of the inwardly-rectifying K<sup>+</sup> channel Kir4.1. *Neurobiol Dis.* 2011;**43**(1):239–247.
13. Rose CR, et al. Evidence that glial cells modulate extracellular pH transients induced by neuronal activity in the leech central nervous system. *J Physiol.* 1994;**481** (Pt 1):1–5.
14. Tsai KL, et al. Mechanism of oxidative stress-induced intracellular acidosis in rat cerebellar astrocytes and C6 glioma cells. *J Physiol.* 1997;**502** (Pt 1):161–174.
15. Gilmore JH. Intracellular pH transients of mammalian astrocytes. *North.* 2008;**29**(10):1883–1889.
16. Hibino H, et al. Differential assembly of inwardly rectifying K<sup>+</sup> channel subunits, Kir4.1 and Kir5.1, in brain astrocytes. *J Biol Chem.* 2004;**279**(42):44065–44073.
17. Olsen ML, et al. Functional implications for Kir4.1 channels in glial biology: from K<sup>+</sup> buffering to cell differentiation. *J Neurochem.* 2008;**107**(3):589–601.
18. Connors NC, et al. The potassium channel Kir4.1 associates with the dystrophin-glycoprotein complex via alpha-syntrophin in glia. *J Biol Chem.* 2004;**279**(27):28387–28392.
19. Connors NC, et al. Potassium channel Kir4.1 macromolecular complex in retinal glial cells. *Glia.* 2006;**53**(2):124–131.
20. Butt AM, et al. Inwardly rectifying potassium channels (Kir) in central nervous system glia: a special role for Kir4.1 in glial functions. *J Cell Mol Med.* 2006;**10**(1):33–44.
21. Nwaobi SE, et al. The role of glial-specific Kir4.1 in normal and pathological states of the CNS. *Acta Neuropathol.* 2016;**132**(1):1–21.
22. Haydon PG, et al. Astrocyte control of synaptic transmission and neurovascular coupling. *Physiol Rev.* 2006;**86**(3):1009–1031. doi:10.1152/physrev.00049.2005
23. Dallérac G, et al. How do astrocytes shape synaptic transmission? Insights from electrophysiology. *Front Cell Neurosci.* 2013;**7**:159.
24. Seifert G, et al. Analysis of astroglial K<sup>+</sup> channel expression in the developing hippocampus reveals a predominant role of the Kir4.1 subunit. *J Neurosci.* 2009;**29**(23):7474–7488.
25. Ohno Y. Astrocytic Kir4.1 potassium channels as a novel therapeutic target for epilepsy and mood disorders. *Neural Regen Res.* 2018;**13**(4):651–652.
26. Cohen S, et al. The relationship between sleep and behavior in Autism Spectrum Disorder (ASD): a review. *J Neurodev Disord.* 2014;**6**:44.
27. Reynolds AM, et al. Sleep and autism spectrum disorders. *Pediatr Clin North Am.* 2011;**58**(3):685–698.
28. Winawer MR, et al.; EPGP Investigators. Genetic effects on sleep/wake variation of seizures. *Epilepsia.* 2016;**57**(4):557–565.
29. Parrino L, et al. Sonno ed epilessia: uno scenario affascinante. *Assoc Ital di Med del Sonno.* 2009;**2**:28.
30. Malow BA. Sleep disorders, epilepsy, and autism. *Ment Retard Dev Disabil Res Rev.* 2004;**10**(2):122–125.
31. Vyazovskiy VV, et al. Triggering slow waves during NREM sleep in the rat by intracortical electrical stimulation: effects of sleep/wake history and background activity. *J Neurophysiol.* 2009;**101**(4):1921–1931.
32. Massimini M, et al. The sleep slow oscillation as a traveling wave. *J Neurosci.* 2004;**24**(31):6862–6870.
33. Riedner BA, et al. Sleep homeostasis and cortical synchronization: III. A high-density EEG study of sleep slow waves in humans. *Sleep.* 2007;**30**(12):1643–1657.
34. Carrier J, et al. Morning and evening-type differences in slow waves during NREM sleep reveal both trait and state-dependent phenotypes. *PLoS One.* 2011;**6**(8):9–12.
35. Murphy M, et al. Source modeling sleep slow waves. *Proc Natl Acad Sci USA.* 2009;**106**(5):1608–1613.
36. Sanchez-Vives MV, et al. Cellular and network mechanisms of rhythmic recurrent activity in neocortex. *Nat Neurosci.* 2000;**3**(10):1027–1034.
37. Beltramo R, et al. Layer-specific excitatory circuits differentially control recurrent network dynamics in the neocortex. *Nat Neurosci.* 2013;**16**(2):227–234.
38. Steriade M, et al. A novel slow (<1 Hz) oscillation of neocortical neurons in vivo: depolarizing and hyperpolarizing components. *J Neurosci.* 1993;**13**(8):3252–3265.
39. Steriade M, et al. Spike-wave complexes and fast components of cortically generated seizures. II. Extra- and intracellular patterns. *J Neurophysiol.* 1998;**80**(3):1456–1479.
40. Contreras D, et al. Voltage-sensitive dye imaging of neocortical spatiotemporal dynamics to afferent activation frequency. *J Neurosci.* 2001;**21**(23):9403–9413.
41. Vyazovskiy VV, et al. Cortical firing and sleep homeostasis. *Neuron.* 2009;**63**(6):865–878.
42. Hill S, et al. Modeling sleep and wakefulness in the thalamocortical system. *J Neurophysiol.* 2005;**93**(3):1671–1698.
43. Vyazovskiy VV, et al. Electrophysiological correlates of sleep homeostasis in freely behaving rats. *Prog Brain Res.* 2011;**193**:17–38.
44. Amzica F, et al. Spatial buffering during slow and paroxysmal sleep oscillations in cortical networks of glial cells in vivo. *J Neurosci.* 2002;**22**(3):1042–1053.
45. Tononi G. Slow wave homeostasis and synaptic plasticity. *J Clin Sleep Med.* 2009;**5**(2 Suppl):S16–S19.
46. Tononi G, et al. Sleep and the price of plasticity: from synaptic and cellular homeostasis to memory consolidation and integration. *Neuron.* 2014;**81**(1):12–34.
47. Esser SK, et al. Sleep homeostasis and cortical synchronization: I. Modeling the effects of synaptic strength on sleep slow waves. *Sleep.* 2007;**30**(12):1617–1630.
48. Bölsterli Heinzle BK, et al. Spike wave location and density disturb sleep slow waves in patients with CSWS (continuous spike waves during sleep). *Epilepsia.* 2014;**55**(4):584–591.
49. Kurth S, et al. Traveling slow oscillations during sleep : a marker of brain connectivity in childhood. *Sleep* 2017;**40**(9). doi:10.1093/sleep/zsx121
50. Sanes JR, et al. Many paths to synaptic specificity. *Annu Rev Cell Dev Biol.* 2009;**25**(1):161–195. doi:10.1146/annurev.cellbio.24.110707.175402
51. Uddin LQ, et al. Dissociable connectivity within human angular gyrus and intraparietal sulcus: evidence from functional and structural connectivity. *Cereb Cortex.* 2010;**20**(11):2636–2646.

52. Campbell IG, et al. Longitudinal trajectories of non-rapid eye movement delta and theta EEG as indicators of adolescent brain maturation. *Proc Natl Acad Sci USA*. 2009;**106**(13):5177–5180.
53. Buchmann A, et al. EEG sleep slow-wave activity as a mirror of cortical maturation. *Cereb Cortex*. 2011;**21**(3):607–615.
54. de Vivo L, et al. Ultrastructural evidence for synaptic scaling across the wake/sleep cycle. *Science*. 2017;**355**(6324):507–510.
55. Zikopoulos B, et al. Changes in prefrontal axons may disrupt the network in autism. *J Neurosci*. 2010;**30**(44):14595–14609.
56. Uddin LQ. Typical and atypical development of functional human brain networks: insights from resting-state fMRI. *Front Syst Neurosci*. 2010;**4**(May):1–12.
57. Hung CS, et al. Local experience-dependent changes in the wake EEG after prolonged wakefulness. *Sleep*. 2013;**36**(1):59–72.
58. Nagai H, et al. Sleep consolidates motor learning of complex movement sequences in mice. *Sleep*. 2016;**40**(2). doi:10.1093/sleep/zsw059
59. Boly M, et al. Altered sleep homeostasis correlates with cognitive impairment in patients with focal epilepsy. *Brain*. 2017;**140**:1026–1040.
60. Huber R, et al. Arm immobilization causes cortical plastic changes and locally decreases sleep slow wave activity. *Nat Neurosci*. 2006;**9**(9):1169–1176.
61. Bellesi M, et al. Effects of sleep and wake on astrocytes: clues from molecular and ultrastructural studies. *BMC Biol*. 2015;**13**:66.
62. Xie L, et al. Sleep drives metabolite clearance from the adult brain. *Science*. 2013;**342**(6156):373–377. doi:10.1126/science.1241224
63. DiNuzzo M, et al. Brain energetics during the sleep-wake cycle. *Curr Opin Neurobiol*. 2017;**47**:65–72.
64. Haydon PG. Astrocytes and the modulation of sleep. *Curr Opin Neurobiol*. 2017;**44**:28–33.
65. Chever O, et al. Implication of Kir4.1 channel in excess potassium clearance: an in vivo study on anesthetized glial-conditional Kir4.1 knock-out mice. *J Neurosci*. 2010;**30**(47):15769–15777.
66. Su BL, et al. Detecting slow wave sleep using a single EEG signal channel. *J Neurosci Methods*. 2015;**243**:47–52.
67. Jaar O, et al. Analysis of slow-wave activity and slow-wave oscillations prior to somnambulism. *Sleep*. 2010;**33**(11):1511–1516.
68. Walacik-Ufnal E, et al. Narcolepsy type 1 and hypersomnia associated with a psychiatric disorder show different slow wave activity dynamics. *Acta Neurobiol Exp (Wars)*. 2017;**77**(2):147–156.
69. Mölle M, et al. Grouping of spindle activity during slow oscillations in human non-rapid eye movement sleep. *J Neurosci*. 2002;**22**(24):10941–10947.
70. Nir Y, et al. Regional slow waves and spindles in human sleep. *Neuron*. 2011;**70**(1):153–169.
71. Destexhe A, et al. The fine structure of slow-wave sleep oscillations: from single neurons to large networks. In: Hutt A, ed. *Sleep and Anesthesia: Neural Correlates in Theory and Experiment*. New York, NY: Springer; 2011:69–105.
72. Fröhlich F, et al. Potassium dynamics in the epileptic cortex: new insights on an old topic. *Neuroscientist*. 2008;**14**(5):422–433.